

# Carbon dots/iron oxide nanoparticles with tuneable composition and properties

Joanna D. Stachowska <sup>1</sup>, Monika B. Gamża <sup>2,3</sup>, Claire Mellor <sup>4</sup>, Ella N. Gibbons <sup>1</sup>, Marta J. Krysmann <sup>1</sup>, Antonios Kelarakis <sup>3\*</sup>, Elżbieta Gumieniczek-Chłopek <sup>5</sup>, Tomasz Strączek <sup>5</sup>, Czesław Kapusta <sup>5</sup>, Anna Sz wajca <sup>6</sup>

1. School of Dentistry, University of Central Lancashire, Preston PR12HE, UK

2. Jeremiah Horrocks Institute for Mathematics, Physics, and Astrophysics, University of Central Lancashire, PR1 2HE, Preston PR12HE, UK

3. UCLan Research Centre for Smart Materials, School of Natural Sciences, University of Central Lancashire, Preston PR12HE, UK

4. School of Psychology and Computer Science, University of Central Lancashire, Preston PR12HE, UK

5. Faculty of Physics and Applied Computer Science, AGH University of Science and Technology, Mickiewicza Ave. 30, Poland, 30-059 Krakow, Poland

6. Adam Mickiewicz University, Faculty of Chemistry, Umultowska 89b, 61-614 Poznań, Poland

\*Correspondence: akelarakis@uclan.ac.uk; Tel.: +44017724172 (A.K.)

Received: date; Accepted: date; Published: date

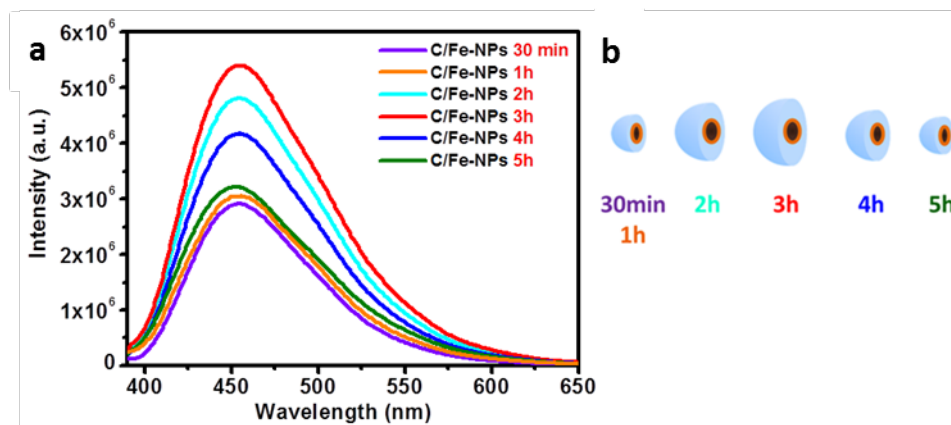


Figure S1. (a) The PL spectra ( $\lambda_{\text{ex}} = 375 \text{ nm}$ ) of aqueous dispersions of C/Fe-NPs prepared from identical reactant mixtures with C/31Fe-NPs, but at various times of pyrolysis (b).

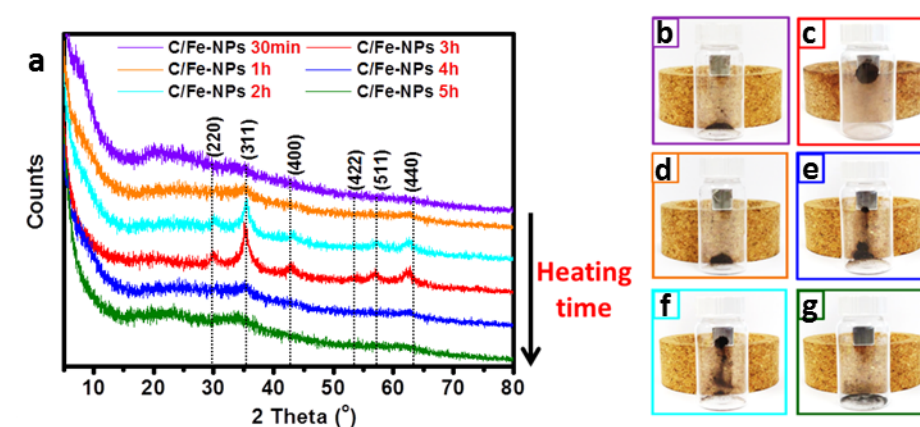


Figure S2. (a) XRD patterns of C/Fe-NPs prepared from identical reactant mixtures with C/31Fe-NPs but at various times of pyrolysis; (b-g) Photos depicting various magnetic properties in the presence of external magnet.

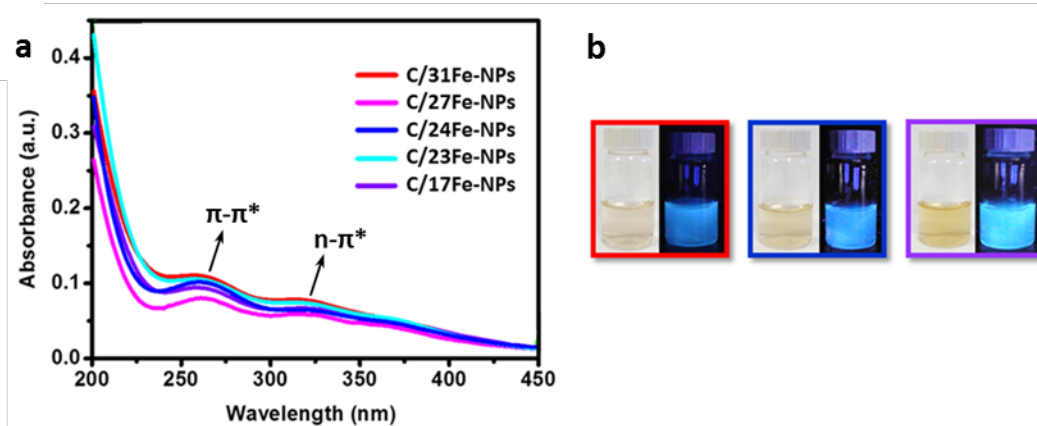


Figure S3. (a) Absorption spectra of aqueous dispersions of 0.01 mg/mL C/Fe-NPs; (b) Photos of C/31Fe-NPs (red), C/24Fe-NPs (blue) and C/17Fe-NPs (purple) under daylight and ultraviolet light.

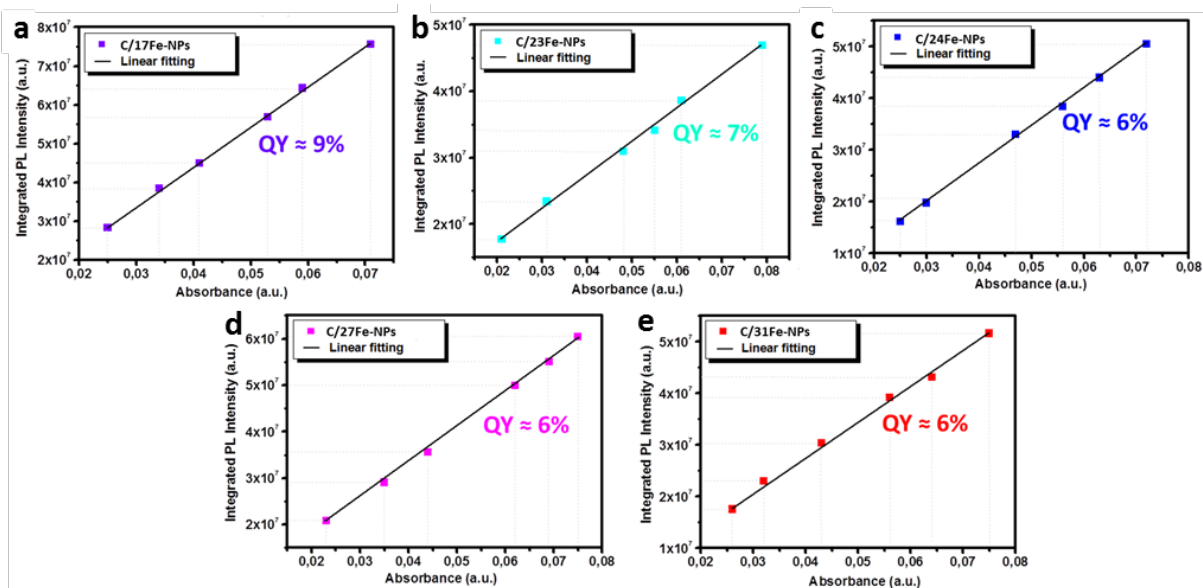


Figure S4. Integrated PL intensity of (a) C/17Fe-NPs, (b) C/23Fe-NPs, (c) C/24Fe-NPs, (d) C/27Fe-NPs and (e) C/31Fe-NPs in water as a function of optical absorbance at 365 nm.

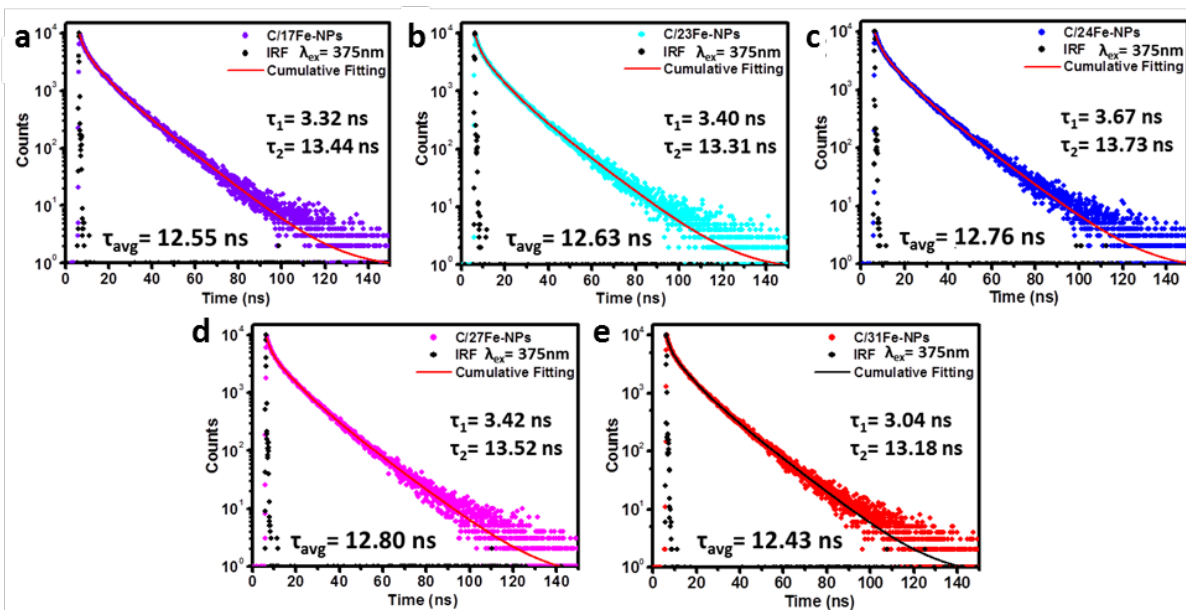


Figure S5. Time-resolved fluorescence decay profiles for aqueous solutions of (a) C/17Fe-NPs, (b) C/23Fe-NPs, (c) C/24Fe-NPs, (d) C/27Fe-NPs, (e) C/31Fe-NPs (E) at  $\lambda_{ex} = 375$  nm.

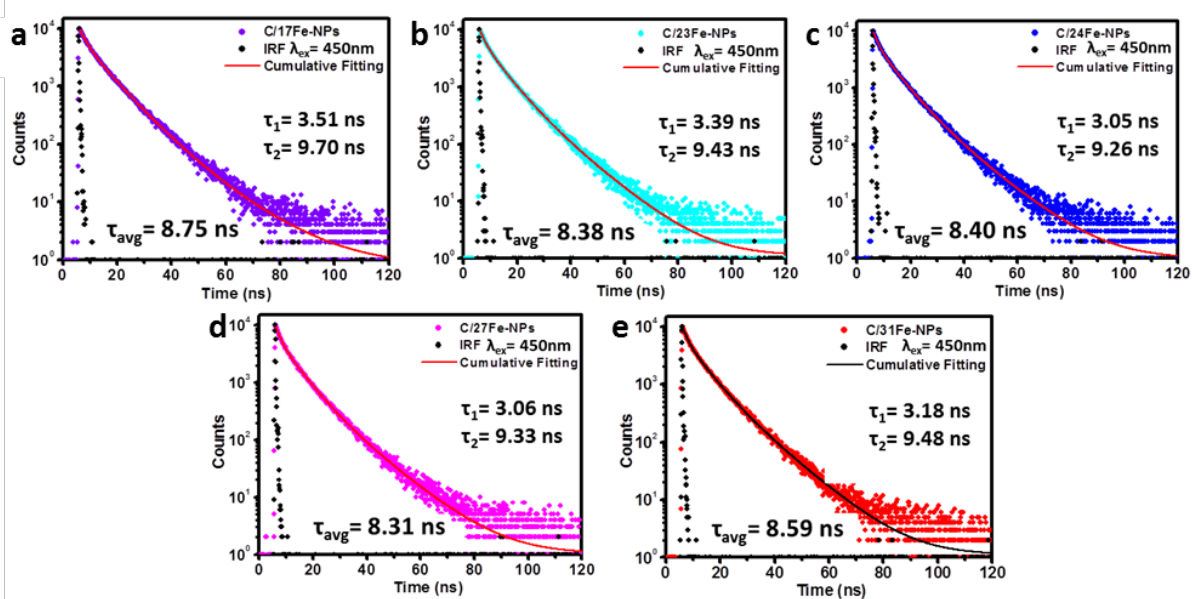


Figure S6. Time-resolved fluorescence decay profiles for aqueous solutions of (a) C/17Fe-NPs, (b) C/23Fe-NPs, (c) C/24Fe-NPs, (d) C/27Fe-NPs, (e) C/31Fe-NPs at  $\lambda_{ex}$  = 450 nm.

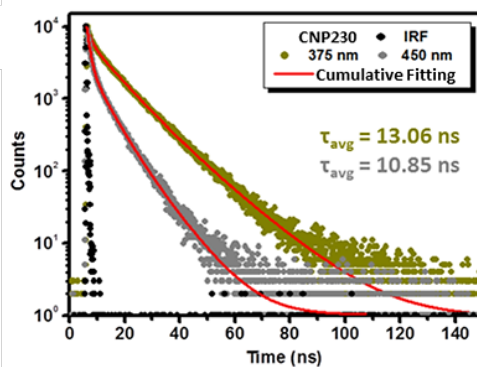


Figure S7. Time-resolved fluorescence decay profiles for aqueous solutions of CNP230 recorded at  $\lambda_{ex}$  = 375 nm (grey colour) and  $\lambda_{ex}$  = 450 nm (dark yellow colour).

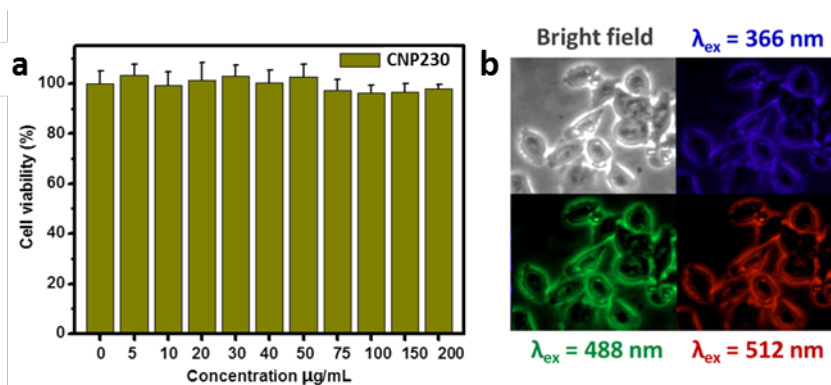


Figure S8. (a) The MTT assay results for HeLa cells incubated with CNP230 for 24 h; (b) The fluorescence microscope images of HeLa cells with internalised CNP230.